

## Origin of Novel Diffusions of Cu and Ag in Semiconductors: The Case of CdTe

Jie Ma and Su-Huai Wei\*

*National Renewable Energy Laboratory, Golden, Colorado 80401, USA*

(Received 17 December 2012; revised manuscript received 8 March 2013; published 4 June 2013)

It is well known in experimental studies that Cu is usually a fast diffuser in semiconductors. In some semiconductors (e.g., CdTe), Ag is also a fast diffuser. The diffusion plays an important role in many applications when Cu (Ag) is employed to tune the semiconductor's electrical or optical properties. However, the origin of why Cu (Ag) shows different diffusion behavior compared to group-IA elements is still unclear. Using first-principles method, we compare the diffusion behaviors between Cu (Ag) and group-IA elements in CdTe, and find that the novel diffusion is due to the strong coupling between Cu (Ag)  $d$  levels and unoccupied host  $s$  levels. This coupling alters the stable doping site, diffusion pathway, and diffusion energy curve from those of group-IA elements, which have no active  $d$  levels, thus making the Cu (Ag) diffusion faster in many semiconductors.

DOI: [10.1103/PhysRevLett.110.235901](https://doi.org/10.1103/PhysRevLett.110.235901)

PACS numbers: 66.30.J-, 61.72.Bb, 61.72.S-, 61.72.uj

Copper (Cu) is an abundant, nontoxic, and easy to purify element that plays an important role in many applications, such as high-temperature superconductors, dilute-magnetic semiconductors, luminescent nanomaterials, and solar cells [1–8]. In many of these applications, the incorporation of Cu is through diffusion [5,9,10]. Experimentally, it has been well known for over 50 years that Cu exhibits fast diffusion in many semiconductors [11,12], including Si [13], Ge [14], GaAs [15], InAs [16], InSb [17], AlSb [18], CdS [19], CdTe [20–22], ZnS [23], and ZnSe [24]. The fast diffusion of Cu has a strong impact on the performance of devices. For example, Cu is widely used as interconnections in integrated circuits, but it must be covered by a barrier metal layer to limit its diffusion; in nanocrystals, the fast diffusion of Cu is helpful for overcoming the dopant solubility [5]; in solar cells, Cu, either as a part of the host material (e.g., Cu chalcogenides) [25,26] or as a dopant to enhance  $p$ -type doping (e.g., CdTe) [10,27–29], can cause the instability of these solar cells.

In spite of its importance, the physical origin for the novel diffusion has not been clearly explained. Here, we study the diffusion behavior of Cu in CdTe and compare it to that of group-IA elements. CdTe is a promising candidate for low-cost thin-film solar cells, which has recently achieved cell-efficiency above 18%. The diffusion of Cu from the back contact into the CdTe absorber is a key process that can significantly enhance solar cell efficiency [9,30,31]. However, the diffusion of Cu into the CdS layer will degrade the efficiency and is linked to long-term device instability [32,33]. The understanding of the diffusion of Cu is thus imperative for further improvement of CdTe solar cells.

Silver (Ag) is another group-IB element that plays an important role in many semiconductors, such as Si, CdSe, InAs [5,34,35]. Experimentally, it is found that Ag diffuses even faster than Cu in CdTe [36], although its size is larger. This is contrary to the common belief that larger atoms

diffuse slower. The abnormal diffusion behavior has not been explained, either.

Using first-principles calculations, we find that the existence of  $d$  electrons is the main reason for the novel diffusion behaviors of Cu and Ag in semiconductors. The effects of  $d$  electrons in group-IB and group-IIB elements in semiconductors have been extensively studied in the past. The  $p$ - $d$  couplings can strongly affect the properties of semiconductors [37]. However, the  $s$ - $d$  coupling has not been carefully considered before, because for most semiconductors with  $O_h$  (diamond structure) or  $T_d$  (zinc-blende structure) symmetry, the coupling between  $s$  and  $d$  levels is not allowed. However, in the diffusion process, the local symmetry around the diffuser is reduced, which can turn on the  $s$ - $d$  coupling. Cu has high-energy  $d$  levels and consequently strong  $s$ - $d$  couplings. We show that the strong  $s$ - $d$  coupling at low-symmetry sites can explain: (i) the most stable interstitial sites of group-IA atoms are the tetrahedral sites, but the most stable site of Cu is the  $M$  site; (ii) all group-IA atoms diffuse along the [111] or equivalent directions from one tetrahedral site to another, but Cu diffusion deviates from exact [111] directions and does not cross the tetrahedral sites; and (iii) the diffusion energy curves of group-IA atoms show two equivalent barriers, but the diffusion energy curve of Cu shows two nonequivalent barriers. Ag has relatively low-energy  $d$  levels and consequently weak  $s$ - $d$  couplings. Therefore, its most stable interstitial site and diffusion pathway are more like those of group-IA atoms, but the  $s$ - $d$  coupling lowers the diffusion energy barrier and can explain its fast diffusion in CdTe.

Our calculations are based on density functional theory within the generalized gradient approximation formulated by Perdew, Burke, and Ernzerhof (PBE) [38] as implemented in the Vienna *ab initio* simulation package (VASP) [39]. The projector augmented wave pseudopotentials [40] are employed, and the valence wave functions are

expanded in a plane-wave basis with an energy cutoff of 300 eV. The calculations are performed in a 64-atom supercell and a  $2 \times 2 \times 2$   $k$ -point mesh is used for Brillouin zone integration. The diffusions are calculated with the nudged elastic band method [41]. Spin polarization has been explicitly taken into account.

First, we discuss the most stable sites of interstitial Cu, Ag, and group-IA atoms in CdTe. Our calculated results are summarized in Table I. The most stable interstitial site for a group-IA atom (Li, Na, or K) is the tetrahedral site. In CdTe (and other zinc-blende materials), there are two kinds of interstitial tetrahedral sites. One is surrounded by cation atoms, which is labeled as  $T_c$ , and the other is surrounded by anion atoms, which is labeled as  $T_a$ . From Table I, we notice that Li prefers the  $T_a$  site, whereas Na and K prefer the  $T_c$  site. From K to Na to Li, the energy difference between the  $T_c$  site and  $T_a$  site increases from  $-0.41$  to  $-0.09$  to  $0.19$  eV. This is explained by the size effect. Because Te gains electrons from Cd, the size of the Te ion is larger than that of the Cd ion. Therefore, there is more space around the  $T_c$  site. In general, large dopants prefer sites with large space and small dopants prefer sites with small space, to reduce the strain energy. Therefore, as the dopant size increases, the  $T_c$  site becomes more preferred than the  $T_a$  site.

Cu has ten  $3d$  electrons. Because the  $d$  electrons are not as localized in the nucleus region as the core electrons, the positive charges in the nucleus are not fully screened by the  $d$  electrons. Therefore, the  $4s$  electron of Cu experiences a strong Coulomb attraction and locates close to the nucleus. As a result, the size of Cu is small, so Cu is more stable at the  $T_a$  site than at the  $T_c$  site.  $\text{Cu}^+$  is further stabilized by stronger Coulomb attraction at the  $T_a$  site. However, according to our density functional calculations, the most stable site of interstitial Cu is not the tetrahedral site. Instead, it is nearly in the middle of the two tetrahedral sites, which is labeled as  $M$  here. The reason is the  $s$ - $d$  coupling between the occupied Cu  $d$  levels and the unoccupied host  $s$  levels. When Cu stays at a tetrahedral site, the local symmetry is  $T_d$ . According to the crystal field splitting, the  $d$  levels split into a triplet  $t_2$  state and a doublet  $e$  state, and the  $s$  level is in a singlet  $a_1$  state. Because the  $d$  levels and  $s$  levels have different symmetries, they cannot couple. However, when Cu moves away

from the tetrahedral site, the symmetry is reduced and the  $s$ - $d$  coupling becomes allowed. The  $s$ - $d$  coupling can be observed clearly from the partial density of states (pDOS) in Fig. 1. Compared to the pDOS at the  $T_c$  site, the occupied Cu  $d$  levels move down in energy at the  $M$  site, and the unoccupied  $s$  levels move up in energy. The system gains the electronic energy from the  $s$ - $d$  coupling. However, the  $M$  site has relatively small space for interstitial atoms compared to the tetrahedral sites, so the strain energy is higher at the  $M$  site. The competition between the electronic energy gain and the strain energy cost determines the relative energies of the  $M$  and tetrahedral sites. Because the size of Cu is small due to the existence of  $d$  electrons, the strain energy cost is small. Furthermore, because the  $d$  levels of Cu are high in energy, the  $s$ - $d$  coupling is strong. Therefore, the electronic energy gain dominates and stabilizes the  $M$  site for interstitial Cu.

The energies of Ag  $d$  electrons are lower than those of Cu. Therefore, the  $s$ - $d$  coupling is weak, and the  $M$  site is higher in energy than the  $T_a$  site. Because the size of Ag is larger than that of Cu, according to the trend discussed above, the energy difference between the  $T_c$  site and  $T_a$  site decreases to 0.08 (0.16) eV for Ag ( $\text{Ag}^+$ ).

Now, we consider the diffusion behavior. The diffusion is calculated from the most stable site to another most stable site. For a group-IA atom, as presented in the right panel of Fig. 2, it diffuses exactly along the  $[111]$  or equivalent directions between the two tetrahedral sites. The diffusion energy curves are presented in the left panel

TABLE I. The energies (eV) of Cu ( $\text{Cu}^+$ ), Ag ( $\text{Ag}^+$ ), and group-IA atoms at the  $M$  and tetrahedral sites. The energy of the most stable site is set to zero.

Atom	$T_a$	$M$	$T_c$
Li	0	0.25	0.19
Na	0.09	0.52	0
K	0.41	0.97	0
Cu ( $\text{Cu}^+$ )	0.12 (0.12)	0 (0)	0.43 (0.63)
Ag ( $\text{Ag}^+$ )	0 (0)	0.06 (0.07)	0.08 (0.16)

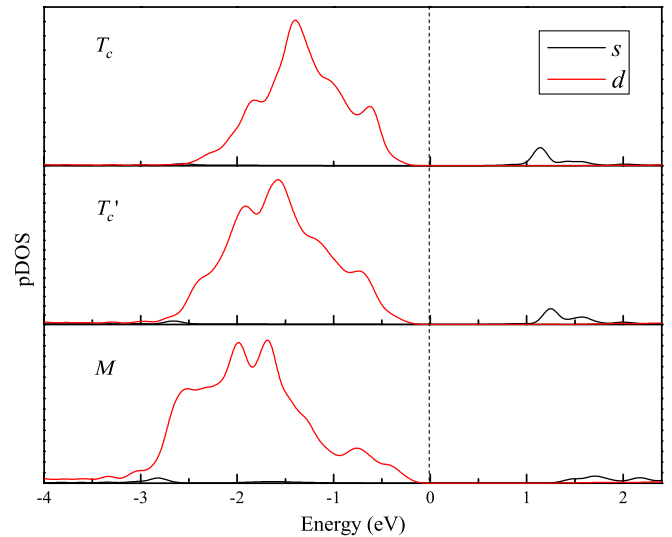


FIG. 1 (color online). The pDOS of  $d$  and  $s$  levels around Cu. The top, middle, and bottom panels are for Cu at the  $T_c$ ,  $T_c'$ , and  $M$  sites, respectively. The energy has been aligned with the  $1s$  core level of CdTe. The dashed line indicates the valence band maximum (VBM) of CdTe. Compared to that at the  $T_c$  site, at the  $T_c'$  and  $M$  sites, the energy of the  $d$  levels below VBM (red line) decreases and the energy of the  $s$  levels above VBM (black line) increases, which indicates the  $s$ - $d$  coupling due to the symmetry reduction.

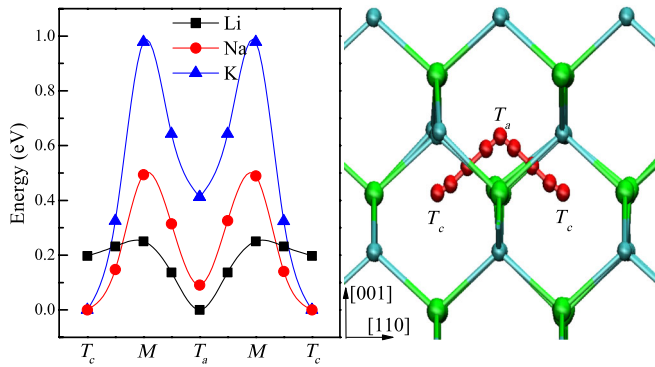


FIG. 2 (color online). The left panel displays the diffusion energy curves of group-IA atoms. The energy of the most stable site is set to zero. The right panel displays the diffusion pathway. The small cyan balls represent Cd, the big green balls represent Te, and the diffusion pathway of interstitial group-IA atom is highlighted in red. The diffusion is exactly along the  $[111]$  and  $[1\bar{1}\bar{1}]$  directions.

of Fig. 2. Due to the lack of  $s$ - $d$  couplings, the strain energy makes the  $M$  site the energy barrier state. The diffusion energy barrier decreases as the atom size decreases. In the diffusion, the group-IA atom passes a metastable site and overcomes two equivalent diffusion barrier states.

The diffusion of Cu is different from those of group-IA atoms. The diffusion pathway and energy curves are presented in Fig. 3. The interstitial Cu first diffuses from the most stable  $M$  site, crossing the  $T_c$  region, to another  $M$  site. However, the second  $M$  site is not related to the first one by a lattice vector. To finish the diffusion, the interstitial Cu then diffuses to the third  $M$  site that is related to the first one by a lattice vector, crossing the  $T_a$  region. In the right panel of Fig. 3, the dashed lines indicate the  $[111]$  and  $[1\bar{1}\bar{1}]$  directions (the diffusion pathway of group-IA

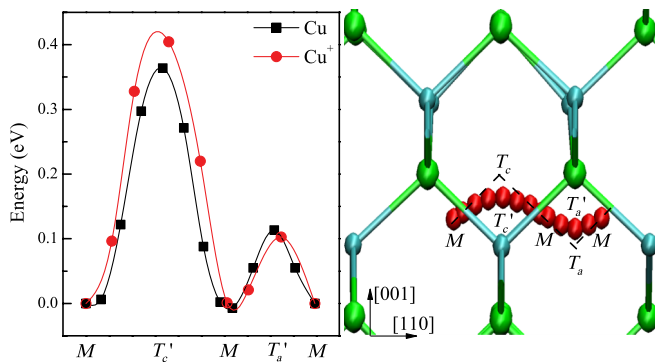


FIG. 3 (color online). The left panel displays the diffusion energy curves of Cu ( $\text{Cu}^+$ ). The energy of the most stable site ( $M$ ) is set to zero. The right panel displays the diffusion pathway. The small cyan balls represent Cd, the big green balls represent Te, and the diffusion pathway of interstitial Cu is highlighted in red. The dashed lines indicate the  $[111]$  and  $[1\bar{1}\bar{1}]$  directions. Different from the group-IA diffusion, the Cu diffusion deviates from these directions and does not cross the tetrahedral sites. The real diffusion barrier states are labeled as  $T_c'$  and  $T_a'$ .

atoms). However, Cu diffusion deviates from these directions, and does not cross the exact  $T_c$  or  $T_a$  site. Instead, it goes through the  $T_c'$  and  $T_a'$  sites labeled in the figure. The deviation from the exact tetrahedral sites is also explained by the  $s$ - $d$  coupling. Although at the exact tetrahedral site, the  $s$ - $d$  coupling is forbidden due to the  $T_d$  symmetry, as Cu moves away from the tetrahedral site, the symmetry is reduced and the  $s$ - $d$  coupling is allowed, which can also be clearly observed from the pDOS (Fig. 1). The deviation from the tetrahedral sites also costs strain energy. The competition between the strain energy cost and the electronic energy gain determines the energies and positions of the  $T_c'$  and  $T_a'$  sites. Because there is more space around the  $T_c$  site, the strain energy cost is small and the  $T_c'$  site is relatively far from the  $T_c$  site with an energy gain of  $\sim 0.07$  eV ( $\sim 0.2$  eV) for Cu ( $\text{Cu}^+$ ). Around the  $T_a$  site, because there is less space, the strain energy cost is larger and almost offsets the electronic energy gain. Therefore, the  $T_a'$  site is close to the  $T_a$  site and the energy gain is only several meV. Different from group-IA diffusions, the  $T_c'$  and  $T_a'$  sites are diffusion barrier states (the left panel of Fig. 3). For Cu ( $\text{Cu}^+$ ), the diffusion energy barrier at the  $T_c'$  site is  $\sim 0.36$  eV ( $\sim 0.42$  eV) and at the  $T_a'$  site is  $\sim 0.11$  eV ( $\sim 0.10$  eV). Therefore, the interstitial Cu crosses two nonequivalent barriers in the diffusion.

The  $s$ - $d$  coupling strength depends on the energy separation between the  $s$  and  $d$  levels. Because PBE calculations underestimate the energy of  $s$  electrons, the band gap is underestimated and the  $s$ - $d$  coupling is overestimated. To correct this error, we employ an empirical external potential to boost the energy of  $s$  electrons so the band gap has the experimental value, following the method in Ref. [42]. The external potential weakens the  $s$ - $d$  coupling and increases the  $s$  orbital size. After applying the potential,

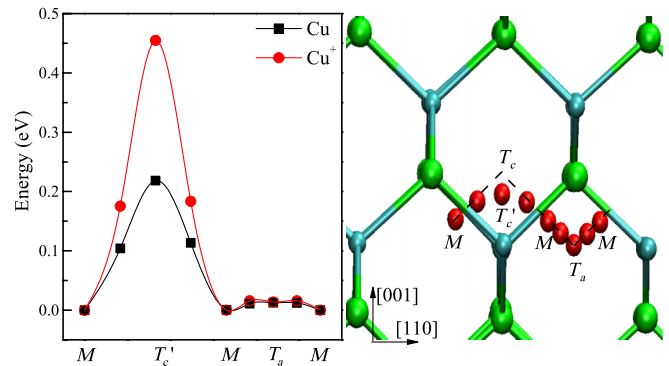


FIG. 4 (color online). The diffusion energy curves (left panel) and pathway (right panel) of Cu ( $\text{Cu}^+$ ) after correcting the band gap. In the left panel, the energy of the most stable site ( $M$ ) is set to zero. In the right panel, the small cyan balls represent Cd, the big green balls represent Te, and the diffusion pathway of interstitial Cu is highlighted in red. The dashed lines indicate the  $[111]$  and  $[1\bar{1}\bar{1}]$  directions. The diffusion pathway shows smaller deviations from these directions, compared to the regular PBE results.

the calculated diffusion pathway and energy curves are displayed in Fig. 4. As expected, the diffusion pathway shows smaller deviations from the [111] direction, compared to the regular PBE results (Fig. 3), because the system gains less electronic energy from the weakened  $s$ - $d$  coupling. Especially in the  $T_a$  region, Cu almost exactly follows the [111] and  $[11\bar{1}]$  directions and crosses the  $T_a$  site. Because the  $s$ - $d$  coupling is weakened, the energy of the  $M$  site increases by  $\sim 0.11$  eV, which is close to that of the  $T_a$  site. Therefore, the diffusion energy curves are almost flat around the  $T_a$  site for Cu ( $\text{Cu}^+$ ). Similarly, the energy of the  $T'_c$  site becomes close to that of the  $T_c$  site. For Cu, the energy barrier at the  $T'_c$  site decreases to  $\sim 0.22$  eV. This is mainly due to the size effect. As the size of the  $s$  orbital increases, the atom size increases, so the energy of the  $T_c$  site decreases compared to that of the  $T_a$  site, according to the energy trend in Table I. For  $\text{Cu}^+$ , because the  $s$  orbital is empty, the size of  $\text{Cu}^+$  does not change, so the size effect does not affect the energy barrier. Because the energies of the  $M$  and  $T'_c$  sites both increase by similar amounts for  $\text{Cu}^+$ , the energy barrier of  $\text{Cu}^+$  does not change compared to the regular PBE results. The calculated energy barrier of  $\text{Cu}^+$  (0.46 eV) is very close to the experimental value (0.57 eV) [21].

Our results and analysis above demonstrate clearly that  $d$  electrons play an important role in Cu diffusion. If the  $s$ - $d$  coupling does not exist, Cu should diffuse similarly as group-IA atoms. In this case, the diffusion barrier state appears around the  $M$  site and the energy barrier is  $E(M) - E(T_a)$ , which is greater than  $E(T_c) - E(T_a)$ . As the  $s$ - $d$  coupling is introduced into the system, the energy of the  $M$  site decreases, thus lowering the energy barrier. In the CdTe case, the  $M$  site becomes degenerate in energy with the  $T_a$  site and the  $T'_c$  site becomes the diffusion barrier state. Furthermore, the  $s$ - $d$  coupling also lowers the energy of the  $T'_c$  site compared to that of the  $T_c$  site. The real energy barrier  $E(T'_c) - E(M)$  is smaller than  $E(T_c) - E(T_a)$ . Therefore, we conclude that the  $s$ - $d$  coupling decreases the diffusion energy barrier and contributes to the fast diffusion of Cu.

For Ag ( $\text{Ag}^+$ ), because the  $s$ - $d$  coupling is weak, the diffusion pathway shows no deviations from the [111] direction; i.e., it is similar to those of group-IA atoms. However, the  $s$ - $d$  coupling still affects the diffusion. Because the  $s$ - $d$  coupling lowers the energy of the  $M$  site, it is not the diffusion barrier state within regular PBE calculations (left panel of Fig. 5). As Ag moves away from tetrahedral sites, the system gains the electronic energy from the  $s$ - $d$  coupling and loses the strain energy. The competition between these two terms makes the diffusion barrier state close to the  $T_c$  site for Ag. For  $\text{Ag}^+$ , because its strain energy is smaller and the electronic energy gain is larger at low-symmetry sites, the diffusion barrier state is  $T_c$ . The diffusion energy barrier is determined by the energy difference between the  $T_c$  and  $T_a$

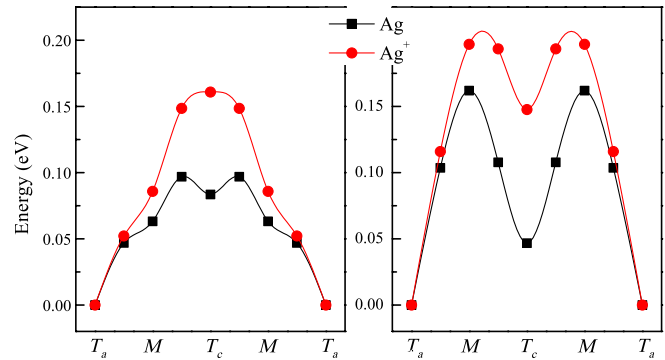


FIG. 5 (color online). The diffusion energy curves of Ag ( $\text{Ag}^+$ ) before (left panel) and after (right panel) correcting the band gap. The energy of the most stable site ( $T_a$ ) is set to zero.

sites, which is smaller than that of Cu. After applying the external potential (right panel of Fig. 5), the  $s$ - $d$  coupling is weakened, so the  $M$  site increases in energy and becomes the diffusion barrier state. However, because the  $s$ - $d$  coupling still exists, the energy of the  $M$  site is close to that of  $T_c$ . The diffusion energy barrier for Ag (0.16 eV) and  $\text{Ag}^+$  (0.2 eV) is smaller than that of Cu, which explains the faster diffusion [36].

In conclusion, we have compared the diffusion behaviors of interstitial Cu and Ag with group-IA atoms. The most stable interstitial sites, diffusion pathways, and diffusion energy curves are very different in these cases. All these differences are explained by the  $s$ - $d$  coupling. The  $s$ - $d$  coupling lowers the diffusion barrier and contributes to the fast diffusion. Because the results and analysis are based mainly on the symmetry argument, we expect that the same conclusion can be obtained for diffusions in other zinc-blende semiconductors.

We are grateful to Juarez L.F. Da Silva for useful discussions. The work at NREL is supported by the U.S. Department of Energy under Contract No. DE-AC36-08GO28308.

\*Corresponding author.  
swei@nrel.gov

- [1] Z. Z. Sheng and A. M. Hermann, *Nature (London)* **332**, 55 (1988).
- [2] R. Q. Wu, G. W. Peng, L. Liu, Y. P. Feng, Z. G. Huang, and Q. Y. Wu, *Appl. Phys. Lett.* **89**, 062505 (2006).
- [3] A. Pandey, S. Brovelli, R. Viswanatha, L. Li, J. M. Pietryga, V. I. Klimov, and S. A. Crooker, *Nat. Nanotechnol.* **7**, 792 (2012).
- [4] L. König, I. Rabin, W. Schulze, and G. Ertl, *Science* **274**, 1353 (1996).
- [5] D. Mocatta, G. Cohen, J. Schattner, O. Millo, E. Rabani, and U. Banin, *Science* **332**, 77 (2011).
- [6] N. S. Karan, D. D. Sarma, R. M. Kadam, and N. Pradhan, *J. Phys. Chem. Lett.* **1**, 2863 (2010).
- [7] F. A. Shirland, *Advanced energy conversion* **6**, 201 (1966).

- [8] I. Repins, M. A. Contreras, B. Egaas, C. DeHart, J. Scharf, C. L. Perkins, B. To, and R. Noufi, *Prog. Photovoltaics* **16**, 235 (2008).
- [9] T. A. Gessert, W. K. Metzger, P. Dippo, S. E. Asher, R. G. Dhere, and M. R. Young, *Thin Solid Films* **517**, 2370 (2009).
- [10] T. A. Gessert, S. Asher, S. Johnston, M. Young, P. Dippo, and C. Corwine, *Thin Solid Films* **515**, 6103 (2007).
- [11] R. N. Hall and J. H. Racette, *J. Appl. Phys.* **35**, 379 (1964).
- [12] M. B. Dutt and B. L. Sharma, *Diffusion in Semiconductors and Non-Metallic Solids* (Springer-Verlag, Berlin, 2003).
- [13] J. D. Struthers, *J. Appl. Phys.* **27**, 1560 (1956).
- [14] C. S. Fuller and J. D. Struthers, *Phys. Rev.* **93**, 1182 (1954).
- [15] C. S. Fuller and J. M. Whelan, *J. Phys. Chem. Solids* **6**, 173 (1958).
- [16] C. Hilsun, *Proc. Phys. Soc. London* **73**, 685 (1959).
- [17] H. J. Stocker, *Phys. Rev.* **130**, 2160 (1963).
- [18] R. H. Wieber, H. C. Gorton, and C. S. Peet, *J. Appl. Phys.* **31**, 608 (1960).
- [19] R. L. Clarke, *J. Appl. Phys.* **30**, 957 (1959).
- [20] E. D. Jones and J. C. Clark, in *Diffusion of Group I, II, and III Impurities in CdTe*, edited by P. Capper, Properties of Narrow Gap Cadmiumbased Compounds, EMIS Data Reviews (INSPEC, London, 1994).
- [21] E. D. Jones, N. M. Stewart, and J. B. Mullin, *J. Cryst. Growth* **117**, 244 (1992).
- [22] H. H. Woodbury and M. Aven, *J. Appl. Phys.* **39**, 5485 (1968).
- [23] T. Lukaszewicz, *Phys. Status Solidi (a)* **73**, 611 (1982).
- [24] T. Lukaszewicz and J. Zmija, *Phys. Status Solidi (a)* **62**, 695 (1980).
- [25] S. Martinuzzi, *Sol. Cells* **5**, 243 (1982).
- [26] R. Herberholz, U. Rau, H. Schock, T. Haalboom, T. Godecke, F. Ernst, C. Beilharz, K. Benz, and D. Cahen, *Eur. Phys. J. Appl. Phys.* **6**, 131 (1999).
- [27] T. A. Gessert, M. J. Romero, R. G. Dhere, and S. E. Asher, *Mater. Res. Soc. Symp. Proc.* **763**, 133 (2003).
- [28] C. R. Corwine, A. O. Pudov, M. Gloeckler, S. H. Demtsu, and J. R. Sites, *Solar Energy Mater. Sol. Cells* **82**, 481 (2004).
- [29] B. E. McCandless and J. R. Sites, *Handbook of Photovoltaic Science and Engineering* (Wiley, West Sussex, England, 2003).
- [30] J. Ma, S.-H. Wei, T. A. Gessert, and K. K. Chin, *Phys. Rev. B* **83**, 245207 (2011).
- [31] F. H. Seymour, V. Kaydanov, T. R. Ohno, and D. Albin, *Appl. Phys. Lett.* **87**, 153507 (2005).
- [32] S. Hegedus, D. Ryan, K. Dobson, B. McCandless, and D. Desai, *Mater. Res. Soc. Symp. Proc.* **763**, B9.5.1 (2003).
- [33] K. D. Dobson, I. Visoly-Fisher, G. Hodes, and D. Cahen, *Solar Energy Mater. Sol. Cells* **62**, 295 (2000).
- [34] A. Sahu, M. S. Kang, A. Kompch, C. Notthoff, A. W. Wills, D. Deng, M. Winterer, C. D. Frisbie, and D. J. Norris, *Nano Lett.* **12**, 2587 (2012).
- [35] F. Rollert, N. A. Stolwijk, and H. Mehrer, *J. Phys. D* **20**, 1148 (1987).
- [36] H. Wolf, F. Wagner, and Th. Wichert (Isolde Collaboration), *Phys. Rev. Lett.* **94**, 125901 (2005).
- [37] S.-H. Wei and A. Zunger, *Phys. Rev. B* **37**, 8958 (1988).
- [38] J. P. Perdew, K. Burke, and M. Ernzerhof, *Phys. Rev. Lett.* **77**, 3865 (1996).
- [39] G. Kresse and J. Furthmuller, *Phys. Rev. B* **54**, 11 169 (1996).
- [40] G. Kresse and D. Joubert, *Phys. Rev. B* **59**, 1758 (1999).
- [41] G. Mills and H. Jonsson, *Phys. Rev. Lett.* **72**, 1124 (1994).
- [42] S. Lany, H. Raebiger, and A. Zunger, *Phys. Rev. B* **77**, 241201(R) (2008).